OUKA
Osaka University Knowledge Archive

Title	Thermal defect healing of single-walled carbon nanotubes assisted by supplying carbon-containing reactants
Author(s)	Wang, Mengyue; Maekawa, Manaka; Shen, Man et al.
Citation	Applied Physics Express. 2023, 16(1), p. 015002
Version Type	AO
URL	https://hdl.handle.net/11094/90046
rights	
Note	

Osaka University Knowledge Archive : OUKA

https://ir.library.osaka-u.ac.jp/

Osaka University

Thermal defect healing of single-walled carbon nanotubes assisted by supplying carbon-containing reactants

Mengyue Wang, [*a] *Manaka Maekawa,* [a] *Man Shen,* [a] *Yuanjia Liu,* [a] *Michiharu Arifuku,* [b] *Noriko Kiyoyanagi,* [b] *Taiki Inoue,* [a] *Yoshihiro Kobayashi*[*a]

[a] Department of Applied Physics, Osaka University, Suita, Osaka 565-0871, Japan

[b] Nippon Kayaku Co., Ltd., 31-12, Shimo 3-chome, Kita-ku, Tokyo 115-8588, Japan

*Email: wang.my@ap.eng.osaka-u.ac.jp, kobayashi@ap.eng.osaka-u.ac.jp

This is the version of the article before peer review or editing, as submitted by an author to Applied Physics Express on October 20th, 2022. IOP Publishing Ltd is not responsible for any errors or omissions in this version of the manuscript or any version derived from it. The Version of Record is available online at https://doi.org/10.35848/1882-0786/acaaec.

Abstract:

We experimentally investigated the effect of carbon-containing reactants (C_2H_2) on healing the defects in single-walled carbon nanotubes (SWCNTs) by thermal processes at high temperatures (~1100^{o}C). Introducing C_2H_2 notably improved the crystallinity of healed SWCNTs compared with the thermal process in Ar ambient without C_2H_2. The defect healing rate increased with increasing C_2H_2 partial pressure and the healing effect of C_2H_2 was more remarkable for relatively thinner SWCNTs (<1.1 nm). Combined with the relevant theoretical works reported previously, we propose the healing model, in which C_2H_2 helps to heal the vacancy defects and increases the healing rate at high temperatures.

Keywords: single-walled carbon nanotubes, defect healing, crystallinity, post treatment, C_2H_2

Carbon nanotubes (CNTs), from their discovery in 1991,[1] have been wildly studied because of their supposed outstanding electronic,[2, 3] optical,[4] and mechanical[5] properties. Especially, compared to multiwalled CNTs (MWCNTs), single-walled CNTs (SWCNTs) becomes one of the potential materials for application in electronics (transistors, interconnects, memory),[6, 7] sensors (optical, biological, chemical),[8, 9] and so on. However, the defects formed in SWCNTs are challenging to be avoided. The existence of defects dramatically degrades the electrical[10-12] and thermal transport[13] and mechanical strength[14, 15] of SWCNTs. Such defects, including adatom,[16] vacancy,[17] pentagon-heptagon pair (5|7),[18, 19] pentagon-heptagon-heptagon-pentagon (5|7/7|5) defects,[20] are not favored thermodynamically due to their high formation energy,[18, 21] but they can be created in the SWCNT growth process [22-24] and chemical post-treatment step.[25] The defects were observed through structure characterization.[26, 27]

High-temperature treatment has been suggested to heal the defects.[28] During the SWCNT growth process, the highly ordered crystalline structure of SWCNTs tends to be found with the increase in the growth temperature.[29] Further theoretical and experimental discussion explained this phenomenon by the temperature-activated catalytic defect healing,[30] which mentioned that simple defects with lower healing activation energy would be more readily cured, such as the 5|7 defects.[18] When talking about the defects created by the electron/photon irradiation, unlike the defects formed in the growth process, experimental evidence indicated that the defective SWCNTs could be healed by annealing under a moderate temperature (1000-2000 ^{o}C) and even at room temperature.[31, 32] Then, the subsequent calculation indicated that, because of the low healing activation energy barrier (~2 eV), the adatom-vacancy defect is a possible candidate of defects generated on the irradiated-nanotubes.[33] Besides, the high temperature was also applied to the post-treatment process to heal the low-temperature synthesized or chemically treated SWCNTs and MWCNTs. For example, treating MWCNTs at 1200–2000 ^{o}C in a high vacuum or at 2000–2800 ^{o}C in an argon (Ar) atmosphere improved crystallinity.[34-36] Similarly, in SWCNT healing, high-temperature treatment (1000–2400 ^{o}C) has also been reported to increase the overall crystallinity by defect aggregation and self-healing of the graphene lattice.[37, 38] Nevertheless, there appears to be a limitation in healing vacancy defects at high temperature. Based on the simulation studies, once the vacancy

defects formed and diffused into nanotubes, even if the vacancy defects could proceed with a self-healing via ring isomerization, it is hard to heal entirely unless foreign carbon atoms are added.[39] In previous studies, as one of the carbon-containing reactants, ethanol has been used as the defect healer in the restoration of graphene oxide.[40, 41] Recently, carbon-containing reactants have been considered as the defect healer in the high-temperature annealing process to heal vacancy defects in CNTs. Until now, simulation studies confirmed that the carbon sources (CO, C_2H_2 and C_2H_4) used for CNT growth are good candidates to heal vacancy defects during high-temperature CNT synthesis.[39, 42-44] Unfortunately, there is still no experimental report on the healing effect of such carbon-containing reactants.

In this research, we experimentally present the healing effect of carbon-containing reactants on the defective SWCNTs. As one of the carbon-containing reactants, C_2H_2 is selected for the defect healing because it does not contain oxygen atoms, which lead to spontaneous formation of oxidants during pyrolysis process and might disturb the healing result. To avoid the formation of additional defects induced by metal catalyst impurities during post-treatment, we selected the metal-free carbon solid nanoparticle originating from nanodiamond (ND) as the SWCNT growth seed.[45, 46] By fixing the healing temperature to 1100 ^{o}C, through Raman spectra characterization, we explored the influence of C_2H_2 partial pressure and healing time on the C_2H_2 added annealing results. Compared with the SWCNTs only healed in Ar ambient, higher crystallinity of SWCNTs is presented with the injection of C_2H_2. Moreover, with the injection of C_2H_2, a significant increase appeared in the healing efficiency of SWCNTs with small diameter. According to these experimental results, we propose that C_2H_2 helps to increase the high-temperature healing efficiency, especially the healing efficiency of thin SWCNTs.

Relatively defective SWCNTs were prepared by lowering growth temperature from the optimized condition in our previous study.[47] As the starting material of growth seeds, ~10 nm diameter purified ND particles were dropped on the ozone-cleaned Si substrates with a 300-nm-thick thermal oxide layer. The ND pretreatment and the SWCNT growth were performed in a quartz tube chamber which is held in a tubular CVD furnace (GE-1000, GII Techno).[47] Before the growth of SWCNTs, the ND was pretreated with the surface-cleaning process (in air for 10 min at 600 °C) and the annealing

procedure (in 85 kPa Ar for 1 h with 20-sccm Ar injection at 1000 °C).[47] After the annealing process, SWCNTs were synthesized for 10 min with a mixture of 10-sccm C_2H_2 (2%)/Ar and 10-sccm Ar. The total pressure was kept at 500 Pa, corresponding to a C_2H_2 partial pressure of 5 Pa. The temperature of the three-zone furnace was set with a gradient, 850-785-750 °C, which corresponds to the temperature of gas mixture preheating, SWCNT growth (substrate temperature), and post heating, respectively.

After the structural characterization of the above synthesized SWCNTs as described later, the heat treatment for the defect healing was proceeded. The annealing temperature was set at 1100 °C to ensure the healing of defects in Ar ambient and the pyrolysis of C_2H_2.[34-36, 48] The healing time was varied from 0 min to 60 min, where the 0 min represents the healing process stopped once the substrate temperature arrived at 1100°C. During the temperature rising process, 250-sccm Ar was injected into the heating ambient. When the temperature arrived at the annealing temperature, the gas flow was switched to a 250-sccm mixture of Ar (235–250 sccm) and C_2H_2 (2%)/Ar (0–5 sccm). The total pressure was kept at 220 Pa, corresponding to a C_2H_2 partial pressure of 0-0.088 Pa. Keeping the injected C_2H_2 at low partial pressure helped to limit the deposition of a-C. Besides, because such partial pressure is much lower than the value needed for the growth of CNTs (0.5 Pa),[47] we exclude the possibility of CNT nucleation during the annealing process. In addition, the same cleaned Si substrates without any growth seeds and SWCNTs were used as a reference (hereafter called blank samples) to compare the amount of amorphous carbon (a-C) deposited directly on them and on the SWCNT samples.

The structure of the SWCNTs before and after the healing process was analyzed by Raman spectroscopy. A Raman spectrometer (LabRAM HR800, HORIBA Jovin Yvon) was used with an excitation wavelength λex of 633 nm. The laser spot size was approximately 0.9 μm, and the laser power was approximately 9 mW at the measurement point. The exposure time of each measurement spot was 1 s for 5 cycles. Raman spectra of 30 randomly selected spots were collected from each sample, and the averaged spectra were used for the analysis. The quality of formed SWCNTs was evaluated using the intensity ratio of the G-band (~1590 cm^{-1}) to the D-band (1330–1360 cm^{-1}), which was represented as I_G/I_D. The SWCNT quantity was evaluated by comparing the intensity ratio

of the G-band (~1590 cm^{-1}) with the Raman peak from Si substrates (~520 cm^{-1}), which was represented as I_G/I_{Si}.

To investigate the healing role of C_2H_2, we analyzed the SWCNT samples annealed at 1100 °C with 0, 0.035, and 0.088 Pa of C_2H_2 injection for different durations (0–60 min). A control experiment was conducted to exclude the possibility of new nucleation of CNTs. As shown in Figure S1, after the pretreated ND at 1100 °C was annealed with C_2H_2 injection, there was no detection of the G-band found on the reference sample, which excluded the possibility of the new growth of SWCNTs. Thus, the increase in the Raman spectra intensity of the annealed SWCNT samples results from the healing effect.

The radial breathing modes (RBMs) of Raman spectra changed with healing time and the partial pressure of C_2H_2 are exhibited in Figure 1 (a). As a representative, G-band and D-band Raman spectra of the SWCNT samples annealed with 0.088 Pa C_2H_2 is also shown in Figure 1(b). Compared with the spectra of the pristine SWCNT sample, the RBM, G-band, and D-band intensity first decreases during the temperature rising process (at 0 min). We suppose the decrease of Raman intensity is because SWCNTs are damaged by the interaction between the substrate and the pristine SWCNTs at high temperature [49]. By prolonging the healing time to 20, 40, and 60 min, as shown in Figure 1 (a) and (b), the intensity of RBM spectra and G-band gradually increased both with and without the use of C_2H_2. Additional healing results of SWCNTs treated with 0.035 and 0.088 Pa for 5 and 10 min are shown in Figure S2. Without the use of carbon-containing reactant, such increase of G-band and RBM intensity at high temperature has been discussed and explained by the healing of defects.[37, 38, 50, 51] In the meantime, the use of C_2H_2 caused a more rapid intensity increase of the RBM peaks at around 210 and 280 cm^{-1}.

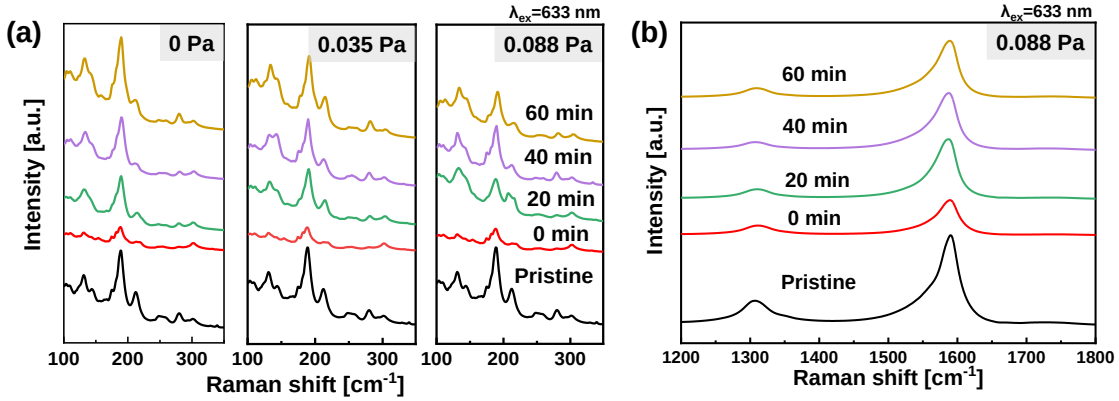

Figure 1: (a) RBM spectra of the pristine SWCNTs and the healed SWCNTs treated with 0, 0.035, and 0.088 Pa C_2H_2 for 0, 20, 40, and 60 min at 1100 °C. (b) G-band and D band of the pristine SWCNTs and the SWCNTs annealed with 0.088 Pa C_2H_2 at 1100 °C for 0, 20, 40, and 60 min.

To further analyze the change of defect density during the healing process, we calculate the I_G/I_D ratio based on the Raman spectra of the healed samples, and the result is presented in Figure 2. The I_G/I_D ratio of the pristine SWCNTs was regarded as the baseline. Compared with the pristine sample, with 0 min healing treatment, the averaged I_G/I_D ratio of the healed SWCNTs did not change much. As the healing time went by, the C_2H_2-injected (0.035 Pa and 0.088 Pa) healing cases gradually expressed higher I_G/I_D ratio than the SWCNTs healed without C_2H_2 injection, which reflects the improvement of SWCNT crystallinity. Moreover, different defect healing rates appeared with changing C_2H_2 partial pressure. According to Figure 2, in 0 and 0.035 Pa C_2H_2 injected annealing process, the defect healing rate was similar in first 20 min and the I_G/I_D ratio increased to around 5.5 in both two cases. After 20 min, the healing rate from 20 min to 60 min slightly decreased in the 0 Pa healing case. Compared with the 0 Pa C_2H_2 injected healing result, although there is a data fluctuation from 20-40 min, a higher overall healing rate from 20 min to 60 min was found in the 0.035 Pa case and the I_G/I_D ratio finally increased to ~8. Further raising the partial pressure of C_2H_2 to 0.088 Pa, a more noticeable increase in healing rate appeared in the first 20 min and the I_G/I_D ratio reached ~8.9 when the healing time was 40 min. Prolonging the healing time to 60 min, we noticed that the I_G/I_D ratio decreased from 40 to 60 min. To analyze this phenomenon, we collected the I_G/I_{Si} ratio of the healed SWCNT samples and the I_D/I_{Si} ratio of the blank samples, shown in Figure S3. From Figure S3(b), the I_G/I_{Si} ratio kept stable for 20 min. On the other hand, the I_D/I_{Si}

ratio of the blank samples gradually increased from 20 to 60 min, representing the deposition of a-C. Thus, we suppose that the decrease in the I_G/I_D ratio is caused by the deposition of a-C in 0.088 Pa-C_2H_2 supplied healing process.

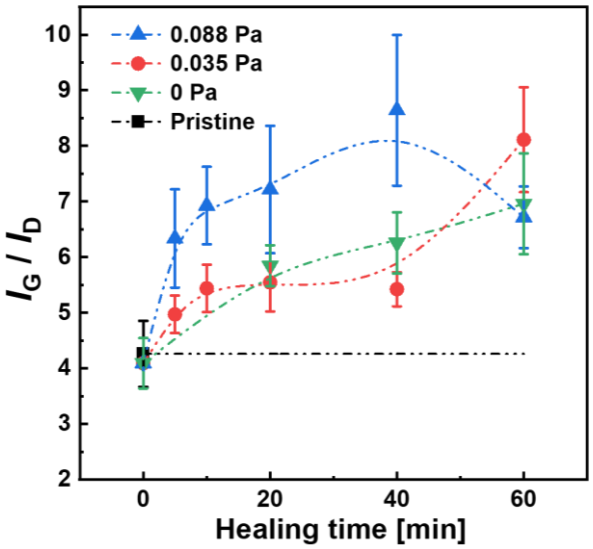

Figure 2: Change in the I_G/I_D ratio of the SWCNTs healed with the injection of C_2H_2 (0, 0.035 and 0.088 Pa) along the healing time. The I_G/I_D ratio of the pristine SWCNTs was plotted as a reference. All dotted lines are guide to the eyes.

Then, we further discuss the influence of C_2H_2 injection to the healing rate of SWCNTs with different diameters. Based on the previous research, the CNT diameter (d_t) is related to the RBM wavenumber (ω_{RBM}) according to the equation:[52)]

$$\omega_{RBM}\ (cm^{-1}) = 223.5\ /d_t\ (nm) + 12.5$$

The relative population of SWCNTs with different diameters can be analyzed based on the peak intensity of the RBM spectra. The high wavenumber (200-300 cm^{-1}) corresponds to the small diameter SWCNTs (<1.1 nm), and the low wavenumber (100–200 cm-1) represents the large diameter SWCNTs (>1.1 nm). Among the RBM spectra shown in Figure 1 (a), significant intensity change appears on the four peaks at around 133, 188, 210, and 280 cm^{-1}, which corresponds to the SWCNTs with 1.8, 1.3, 1.1 and 0.8 nm diameter, respectively. Taking the RBM peaks of SWCNTs with the four diameters as the representative, the healing rates with or without the injection of C_2H_2 are determined as shown in Figure 3. The healing rate was calculated by the changes in the corresponding

RBM peak intensity along the healing time. We divided the intensity change in the RBM peaks from 0 min to 40 min by the duration to exclude the contribution of the a-C deposition in long annealing time, which affects the intensity of Raman spectra. The related details of normalized RBM intensity varied with the healing time are exhibited in Figure S4. Based on previous works,[18, 53, 54] low formation energy of vacancy and 5|7 defects appears in the SWCNTs with small diameter, which eases the formation of these types of defects in the SWCNTs with small diameter. Healing of thin SWCNTs with higher density of defects, especially the vacancy defect, would take longer time compared with thick SWCNTs. Thus, without the injection of C_2H_2, as shown in Figure 3, higher healing rate is found in the SWCNTs with large diameter. When C_2H_2 was added to the healing process, the healing rate of the thick SWCNTs (>1.1 nm) slightly increased. Interestingly, in the SWCNTs with small diameters (<1.1 nm), the healing rate was significantly increased with the use of C_2H_2. These increase in the healing rate confirms that the injection of C_2H_2 during the healing process helped to enhance the defect healing rate, especially to the defects in the SWCNTs with small diameter.

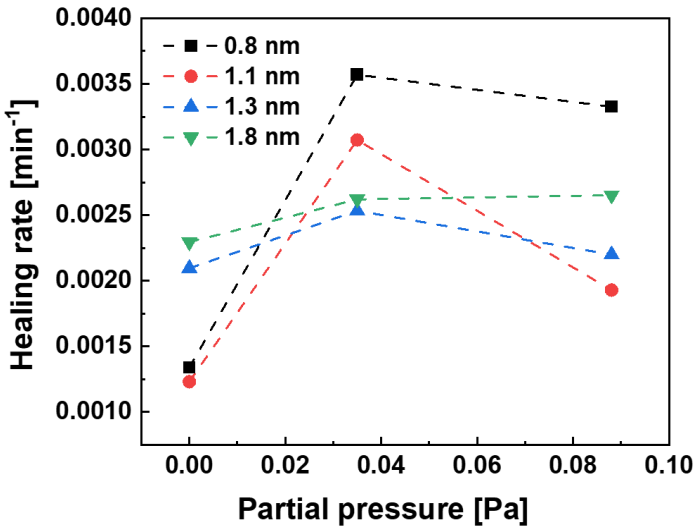

Figure 3: Change of the healing rate with the injection of C_2H_2 (0, 0.035 and 0.088 Pa) for the SWCNTs with different diameter (0.8, 1.1, 1.3, and 1.8 nm).

Based on the aforementioned results of C_2H_2 injected defect healing, we derived the healing behavior of C_2H_2 in the high temperature annealing process and schematically depicted it in Figure 4. For the pristine SWCNTs synthesized at low temperature, several kinds of defects formed during the growth process, including the adatom, vacancy, 5|7

defects, and so on. During the healing process, with the presence of trace amount of oxidative gas impurities (O_2, H_2O, or CO_2), the adatom defects could be partly healed through etching reaction.[55] However, if there are no carbon atoms injected into the healing process, vacancy defects tend to stay or change to closed lattice structures with pentagon and heptagon defects through Stone-Wales-type transformation,[56, 57] which means the difficulty in healing vacancy defects. To heal vacancy defects, the use of carbon-containing reactant is effective because carbon atoms from the reactant are adsorbed on the vacancy defects and incorporated into the lattice of the SWCNTs.[39, 42-44] Thus, in Figure 4, we suppose that the adatom defects and the vacancy defects would be the representative defects which can be healed in the C_2H_2-injected healing process.

Among such defects, the low formation energy of adatom defect makes it easy to be constructed.[53] Thus, compared to the adatom defects, the vacancy defects in the pristine SWCNT structure appear with lower density because of their high formation energy.[53] Besides, related to the diameter of SWCNTs, the formation energy of defects is lower in the SWCNTs with small diameter compared with the one with large diameter,[18, 54] which makes vacancy defects easier to form on the thin SWCNTs. Therefore, as shown in Figure 4, higher-density vacancy defects appear in the pristine SWCNTs with small diameter.

When only heated in Ar gas with low pressure, the adatom defects tend to be healed while the vacancy defects are more likely to stay. On the other hand, when C_2H_2 was added, the vacancy defects could be better healed, which caused an increase in the healing rate in both thick and thin SWCNTs. In this high temperature treatment, the pyrolysis reaction of C_2H_2 also happens, which produced H_2 and helped to remove adatom defects.[55] Moreover, the high density of defects on the thin tube structure would take longer time and be harder to heal, which brings about the low healing rate in thin SWCNTs with high-density defects. Especially for the thin SWCNTs, the healing rate was more drastically increased compared to the thick tubes.

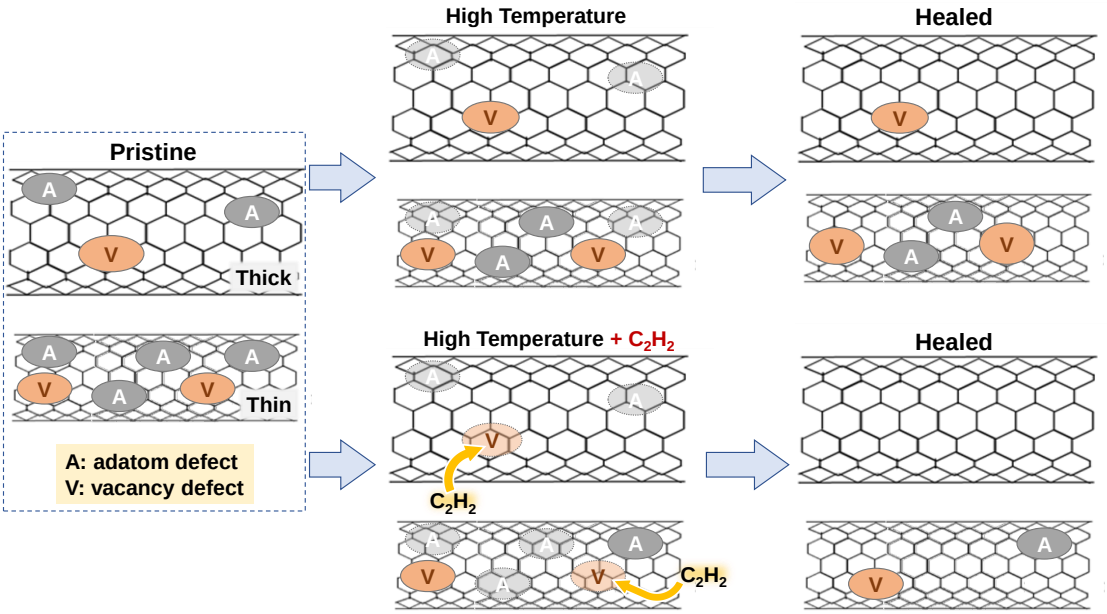

Figure 4: Schematic defect healing diagram of the pristine SWCNTs annealed at high temperature (1100 °C) with or without the injection of C_2H_2. The pristine SWCNTs are divided into thick (>1.1 nm) and thin (<1.1nm) SWCNTs according to their diameter.

Besides, we also investigated the healing effect of ethylene (C_2H_4). As shown in Figure S5, the injection of C_2H_4 resulted in the efficient healing of SWCNTs similarly to the case of C_2H_2, indicating the general effectiveness of carbon-containing reactants in thermal defect healing.

In conclusion, with the experimental results, we confirmed the healing behavior of C_2H_2 in the high temperature (1100 °C) annealing process, which had been only analyzed through theoretical methods. Compared with the SWCNTs healed only in Ar gas, the SWCNTs healed with C_2H_2 presented higher crystallinity. The defect healing rate was increased with rising the partial pressure of injected C_2H_2 from 0 to 0.088 Pa. On the other hand, with the increase of the injected C_2H_2, the formation of a-C for long process time becomes a problem that needs to be solved in future work. Further, considering the diameter of SWCNTs, we found that the healing effect of C_2H_2 injection was more evident in the SWCNTs with small diameter (<1.1 nm). Combining with the previous simulation research about the healing behavior of C_2H_2, we consider that C_2H_2 helps to heal the vacancy defects and increased the high temperature healing rate. Moreover, we

also found that C_2H_4 exhibited a healing ability which is similar to C_2H_2. These results prove that injecting carbon-containing reactants, like C_2H_2, would be an additional important factor for healing SWCNT defects with high efficiency. With the assistance of such carbon-containing reactants, SWCNTs with higher crystallinity can be achieved by the post treatment process, which would further realize the improvement of SWCNT properties required for electronic, thermal, and mechanical applications.

Notes

The authors declare no competing financial interest.

Acknowledgement

The part of this work was finantially supported by JSPS KAKENHI (Grant Numbers JP15H05867 and JP17H02745). This work was also supported by Nanotechnology Platform of MEXT (Grant Number JPMXP09F20OS0002).

References

1) S. Iijima, *Nature* **354**, 56 (1991).
2) A. Lekawa-Raus, J. Patmore, L. Kurzepa, J. Bulmer, K. Koziol, *Adv. Funct. Mater.* **24**, 3661 (2014).
3) G. D. Nessim, *Nanoscale* **2**, 1306 (2010).
4) M. J. O'Connell, S. M. Bachilo, C. B. Huffman, V. C. Moore, M. S. Strano, E. H. Haroz, K. L. Rialon, P. J. Boul, W. H. Noon, C. Kittrell, J. Ma, R. H. Hauge, R. B. Weisman, R. E. Smalley, *Science* **297**, 593 (2002).

5) Y. Bai, H. Yue, R. Zhang, W. Qian, Z. Zhang, F. Wei, *Acc. Mater. Res.* **2**, 998 (2021).
6) A. D. Franklin, M. Luisier, S.-J. Han, G. Tulevski, C. M. Breslin, L. Gignac, M. S. Lundstrom, W. Haensch, *Nano Lett.* **12**, 758 (2012).
7) R. Seidel, A. P. Graham, E. Unger, G. S. Duesberg, M. Liebau, W. Steinhoegl, F. Kreupl, W. Hoenlein, W. Pompe, *Nano Lett.* **4**, 831 (2004).
8) J. Kong, N. R. Franklin, C. Zhou, M. G. Chapline, S. Peng, K. Cho, H. Dai, *Science* **287**, 622 (2000).
9) T. Yamada, Y. Hayamizu, Y. Yamamoto, Y. Yomogida, A. Izadi-Najafabadi, D. N. Futaba, K. Hata, *Nat. Nanotechnol.* **6**, 296 (2011).
10) J. C. Charlier, T. W. Ebbesen, P. Lambin, *Phys. Rev. B* **53**, 11108 (1996).
11) H. J. Choi, J. Ihm, S. G. Louie, M. L. Cohen, *Phys. Rev. Lett.* **84**, 2917 (2000).
12) S. Suzuki, Y. Kobayashi, *Jpn. J. Appl. Phys.* **44**, L1498 (2005).
13) T. Yamamoto, K. Watanabe, *Phys. Rev. Lett.* **96**, 255503 (2006).
14) M. Sammalkorpi, A. Krasheninnikov, A. Kuronen, K. Nordlund, K. Kaski, *Phys. Rev. B* **70**, 245416 (2004).
15) X. Shi, X. He, L. Sun, X. Liu, *Nanoscale Res. Lett.* **17**, 15 (2022).
16) L. Tsetseris, S. T. Pantelides, *Carbon* **47**, 901 (2009).
17) J. Y. Huang, F. Ding, B. I. Yakobson, *Phys. Rev. B* **78**, 155436 (2008).
18) Q. Yuan, Z. Xu, B. I. Yakobson, F. Ding, *Phys. Rev. Lett.* **108**, 245505 (2012).
19) L. Vicarelli, S. J. Heerema, C. Dekker, H. W. Zandbergen, *ACS Nano* **9**, 3428 (2015).
20) E. Ertekin, D. C. Chrzan, M. S. Daw, *Phys. Rev. B* **79**, 155421 (2009).
21) L. G. Zhou, S. Q. Shi, *Appl. Phys. Lett.* **83**, 1222 (2003).
22) Y. Xia, Y. Ma, Y. Xing, Y. Mu, C. Tan, L. Mei, *Phys. Rev. B* **61**, 11088 (2000).
23) J. C. Burgos, E. Jones, P. B. Balbuena, *J. Phys. Chem. C* **118**, 4808 (2014).
24) W. Qian, T. Liu, F. Wei, Z. Wang, G. Luo, H. Yu, Z. Li, *Carbon* **41**, 2613 (2003).
25) M. C. Hersam, *Nat. Nanotechnol.* **3**, 387 (2008).
26) A. V. Krasheninnikov, F. Banhart, *Nat. Mater.* **6**, 723 (2007).
27) K. Suenaga, H. Wakabayashi, M. Koshino, Y. Sato, K. Urita, S. Iijima, *Nat. Nanotechnol.* **2**, 358 (2007).

28) P. Vinten, P. Marshall, J. Lefebvre, P. Finnie, *J. Phys. Chem. C* **117**, 3527 (2013).
29) C. J. Lee, J. Park, Y. Huh, J. Yong Lee, *Chem. Phys. Lett.* **343**, 33 (2001).
30) R. Zhang, Y. Zhang, F. Wei, *Acc. Chem. Res.* **50**, 179 (2017).
31) S. Suzuki, Y. Kobayashi, *J. Phys. Chem. C* **111**, 4524 (2007).
32) S. Suzuki, K. Yamaya, Y. Homma, Y. Kobayashi, *Carbon* **48**, 3211 (2010).
33) S. Okada, *Chem. Phys. Lett.* **447**, 263 (2007).
34) D. Mattia, M. P. Rossi, B. M. Kim, G. Korneva, H. H. Bau, Y. Gogotsi, *J. Phys. Chem. B* **110**, 9850 (2006).
35) R. Jin, Z. X. Zhou, D. Mandrus, I. N. Ivanov, G. Eres, J. Y. Howe, A. A. Puretzky, D. B. Geohegan, *Phys. B* **388**, 326 (2007).
36) J. Zhao, Y. Zhang, Y. Su, X. Huang, L. Wei, E. S.-W. Kong, Y. Zhang, *Diamond Relat. Mater.* **25**, 24 (2012).
37) M. Yudasaka, H. Kataura, T. Ichihashi, L. C. Qin, S. Kar, S. Iijima, *Nano Lett.* **1**, 487 (2001).
38) M. Yudasaka, T. Ichihashi, D. Kasuya, H. Kataura, S. Iijima, *Carbon* **41**, 1273 (2003).
39) T. Nongnual, J. Limtrakul, *J. Phys. Chem. C* **115**, 4649 (2011).
40) K. K. H. De Silva, H. H. Huang, S. Suzuki, R. Badam, M. Yoshimura, *Jpn. J. Appl. Phys.* **57**, 08NB03 (2018).
41) C. Y. Su, Y. Xu, W. Zhang, J. Zhao, A. Liu, X. Tang, C. H. Tsai, Y. Huang, L. J. Li, *ACS Nano* **4**, 5285 (2010).
42) B. Xiao, J. X. Zhao, Y. H. Ding, C. C. Sun, *ChemPhysChem* **11**, 3505 (2010).
43) B. Xiao, X. F. Yu, Y. H. Ding, *J. Mol. Model.* **20**, 2125 (2014).
44) R. L. Zhou, H. Y. He, B. C. Pan, *Phys. Rev. B* **75**, 113401 (2007).
45) D. Takagi, Y. Kobayashi, Y. Homma, *J. Am. Chem. Soc.* **131**, 6922 (2009).
46) Y. Homma, H. Liu, D. Takagi, Y. Kobayashi, *Nano Res.* **2**, 793 (2009).
47) M. Wang, K. Nakamura, M. Arifuku, N. Kiyoyanagi, T. Inoue, Y. Kobayashi, *ACS Omega* **7**, 3639 (2022).
48) N. Matsumoto, A. Oshima, G. Chen, M. Yudasaka, M. Yumura, K. Hata, D. N. Futaba, *Carbon* **87**, 239 (2015).
49) P. Nemes-Incze, G. Magda, K. Kamarás, L. P. Biró, *Nano Res.* **3**, 110 (2010).

50) L. G. Cançado, A. Jorio, E. H. M. Ferreira, F. Stavale, C. A. Achete, R. B. Capaz, M. V. O. Moutinho, A. Lombardo, T. S. Kulmala, A. C. Ferrari, *Nano Lett.* **11**, 3190 (2011).

51) Y. Yang, C. Ramirez, X. Wang, Z. Guo, A. Tokranov, R. Zhao, I. Szlufarska, J. Lou, B. W. Sheldon, *Carbon* **115**, 402 (2017).

52) S. M. Bachilo, M. S. Strano, C. Kittrell, R. H. Hauge, R. E. Smalley, R. B. Weisman, *Science* **298**, 2361 (2002).

53) F. Ding, *Phys. Rev. B* **72**, 245409 (2005).

54) A. J. Lu, B. C. Pan, *Phys. Rev. Lett.* **92**, 105504 (2004).

55) L. Tsetseris, S. T. Pantelides, *J. Phys. Chem. B* **113**, 941 (2009).

56) F. Börrnert, S. Gorantla, A. Bachmatiuk, J. H. Warner, I. Ibrahim, J. Thomas, T. Gemming, J. Eckert, G. Cuniberti, B. Büchner, M. H. Rümmeli, *Phys. Rev. B* **81**, 201401 (2010).

57) G. D. Lee, C. Z. Wang, E. Yoon, N. M. Hwang, D. Y. Kim, K. M. Ho, *Phys. Rev. Lett.* **95**, 205501 (2005).

Supporting information

Thermal defect healing of single-walled carbon nanotubes assisted by supplying carbon-containing reactants

Mengyue Wang, [*a] *Manaka Maekawa,* [a] *Man Shen,* [a] *Yuanjia Liu,* [a] *Michiharu Arifuku,* [b]

Noriko Kiyoyanagi, [b] *Taiki Inoue,* [a] *Yoshihiro Kobayashi*[*a]

[a] Graduate school of engineering, Osaka University, Suita, Osaka 565-0871, Japan

[b] Nippon Kayaku Co., Ltd., 31-12, Shimo 3-chome, Kita-ku, Tokyo 115-8588, Japan

*Email: kobayashi@ap.eng.osaka-u.ac.jp

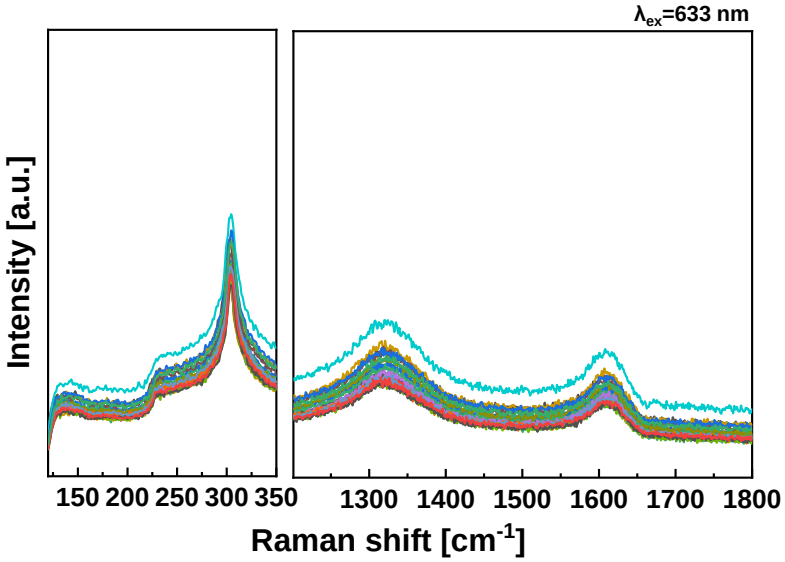

Figure S1: Raman spectra of the nanodiamond (ND) sample treated with the same thermal process as SWCNT growth but without the injection of carbon source and then the healing process (heated at 1100 °C for 60 min with 0.088 Pa C_2H_2 injection).

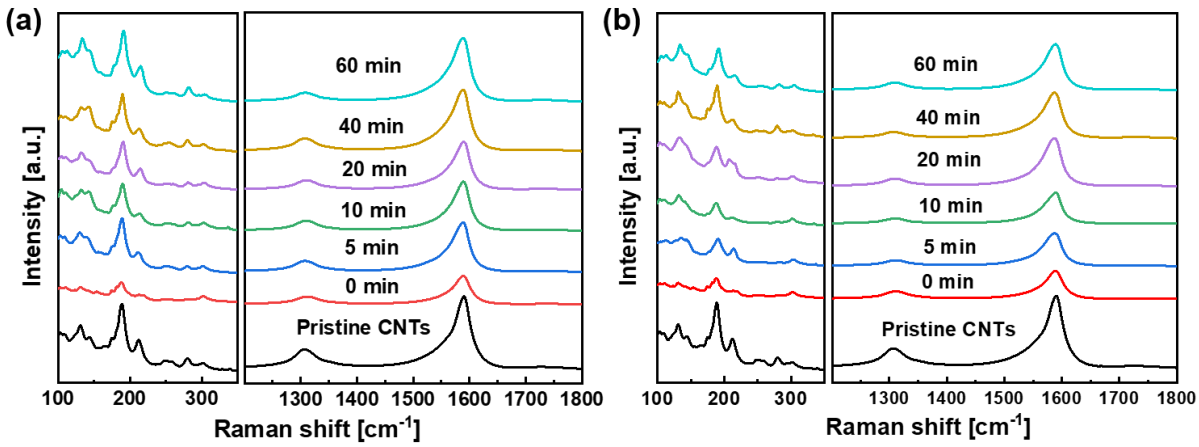

Figure S2: Raman spectra of the pristine SWCNTs and the healed SWCNTs treated with (a) 0.035, and (b) 0.088 Pa C_2H_2 for 0, 5, 10, 20, 40, and 60 min at 1100 °C.

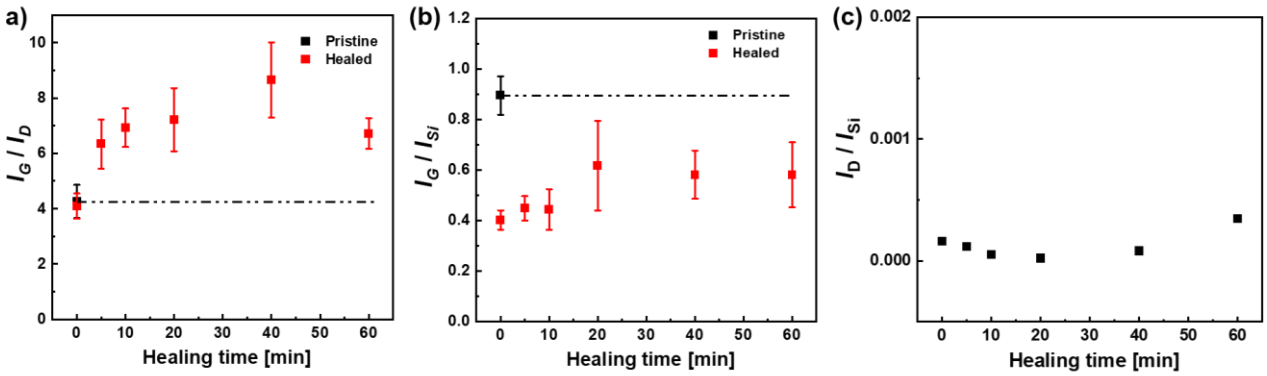

Figure S3: Process time dependence of the (a) I_G/I_D ratio and (b) I_G/I_{Si} ratio of the SWCNTs, and (c) the I_D/I_{Si} ratio of the relevant blank sample treated with the C_2H_2-injected healing process (0.088 Pa). The I_G/I_D and I_G/I_{Si} ratios of the pristine SWCNTs were plotted as a reference.

.

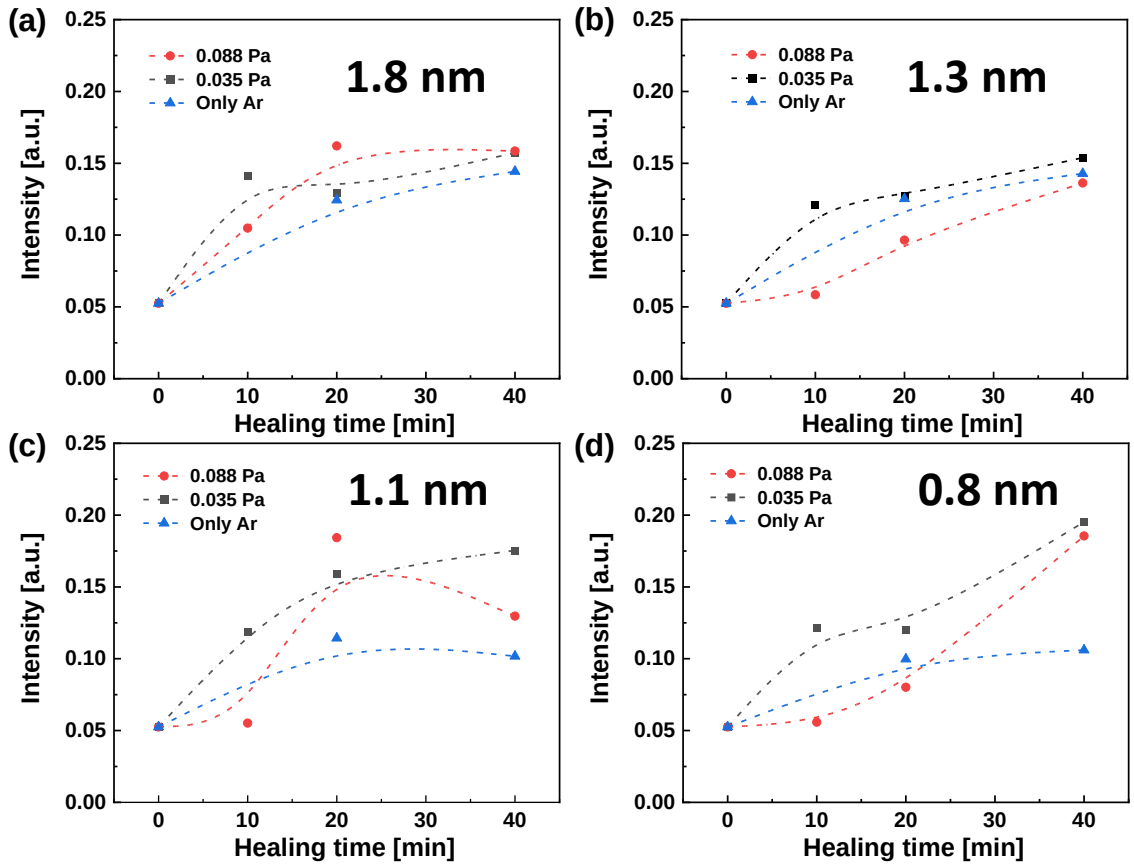

Figure S4: The changes in the RBM peak intensity along the healing time (0, 10, 20, and 40 min). The four representative RBM peaks correspond to the SWCNTs with different diameter: (a) 1.8, (b) 1.3, (c) 1.1, and (d) 0.8 nm.

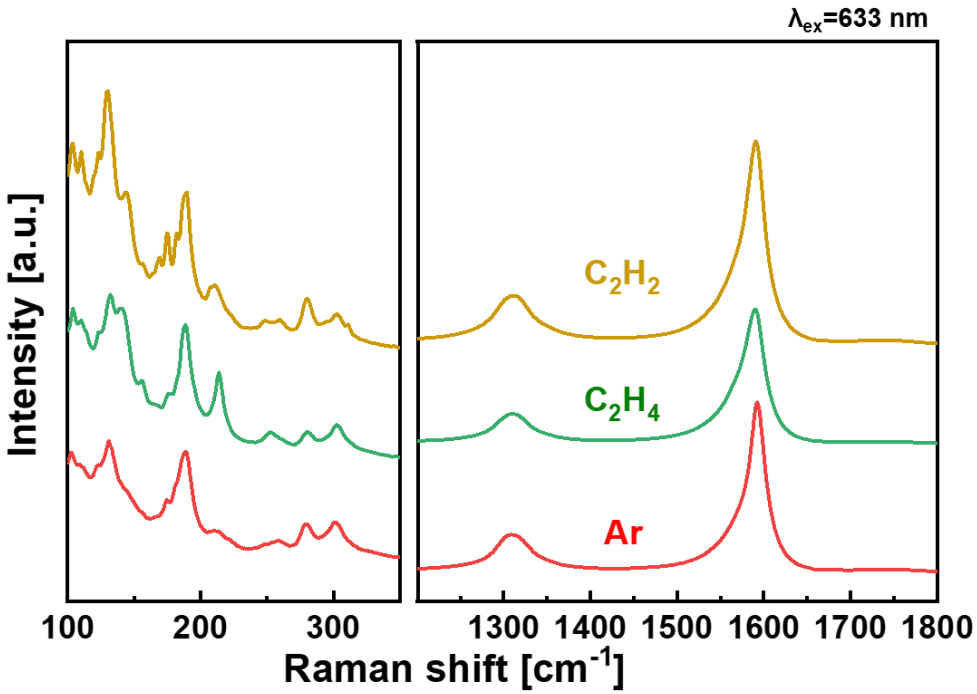

Figure S5: Raman spectra of the healed SWCNTs treated with only Ar, 0.352 Pa C_2H_2 and 0.352 Pa C_2H_4 for 60 min at 1100 ºC.